

# Elucidation on the Effect of Operating Temperature to the Transport Properties of Polymeric Membrane Using Molecular Simulation Tool

Serene Sow Mun Lock<sup>1</sup>, Kok Keong Lau<sup>1</sup>(✉),  
Al-Ameerah Binti Mash'al<sup>1</sup>, Azmi Muhammad Shariff<sup>1</sup>,  
Yin Fong Yeong<sup>1</sup>, Irene Lock Sow Mei<sup>2</sup>, and Faizan Ahmad<sup>3</sup>

<sup>1</sup> Department of Chemical Engineering, Research Center for CO<sub>2</sub> Capture, Universiti Teknologi PETRONAS, 32610 Seri Iskandar, Perak, Malaysia  
serenelock168@gmail.com, alameerah.mashal@gmail.com,  
{laukokkeong, azmish, yinfong.yeong}@utp.edu.my

<sup>2</sup> Process Department, Group Technical Solutions, Project Delivery and Technology Division, PETRONAS, Kuala Lumpur, Malaysia  
irene.lock@petronas.com.my

<sup>3</sup> School of Science and Engineering, Teesside University, Middlesbrough, UK  
f.ahmad@tees.ac.uk

**Abstract.** Existing reports of gas transport properties within polymeric membrane as a direct consequence of operating temperature are in a small number and have arrived in diverging conclusion. The scarcity has been associated to challenges in fabricating defect free membranes and empirical investigations of gas permeation performance at the laboratory scale that are often time consuming and costly. Molecular simulation has been proposed as a feasible alternative of experimentally studied materials to provide insights into gas transport characteristic. Hence, a sequence of molecular modelling procedures has been proposed to simulate polymeric membranes at varying operating temperatures in order to elucidate its effect to gas transport behaviour. The simulation model has been validated with experimental data through satisfactory agreement. Solubility has shown a decrement in value when increased in temperature (an average factor of 1.78), while the opposite has been observed for gas diffusivity (an average factor of 1.32) when the temperature is increased from 298.15 K to 323.15 K. In addition, it is found that permeability decreases by 1.36 times as the temperature is increased.

**Keywords:** Molecular simulation · Polymeric membranes · Transport properties · Operating temperatures

## 1 Introduction

Natural gas is defined as the gaseous fossil fuel that is rich with hydrocarbon occurring naturally underground as is utilized as fuels for petrochemical plants [1]. It is a source of energy for heating, cooking in homes, generating electricity and also vehicles' fuels

[2]. Before supplying to users all over the world, the natural gas has to be treated by removing all unwanted residual gases, e.g. acid gases ( $\text{CO}_2$ ), inert gases ( $\text{N}_2$ ) and oxidizers ( $\text{O}_2$ ), prior to entering the pipeline to obtain highly concentrated methane ( $\text{CH}_4$ ) that constitutes to its actual heating value [3, 4]. Polymeric membranes play a pivotal role in gas separation applied in industrial application attributed to their various advantages, such as occupying a relatively smaller footprint, chemical free, cost effective, high process flexibility, simplicity and high energy efficiency [5]. In typical natural gas processing, the entering natural gas are in the range of 30 °C to 50 °C in order to suit the temperature for membrane separation [6].

A number of existing reports shows that a mere minor changes or fluctuations in operating temperature has affected the transport performance and selectivity of the membrane [7]. Although there have been a lot of studies related to membrane technology, the issue of temperature dependent phenomena onto membrane remains an unclear cut and unexplored. Majority of the experimental data have been confined to gas transport in polymer films at temperatures near 25 or 35 °C, which is devoted to measurement at ambient operating condition, attributed to challenges and cost to control the operating temperatures at different ranges [7].

Rising effort has emerged to elucidate the temperature dependent gas transport behavior of penetrants through membrane. Koros and Paul reported the  $\text{CO}_2$  sorption in poly (ethylene terephthalate) (PET) from 25 to 115 °C, while fitting the values to dual mode sorption model [8]. The gas permeabilities and solubilities of five different gases are reported for bisphenol-A polycarbonate (PC), tetramethyl polycarbonate (TMPC), and tetramethyl hexafluoro polycarbonate (TMHFPC) at temperatures up to 200 °C [7]. Costello and Koros studied the same transport properties in meta/para-isomers of hexafluoroisopropylidene-containing polyimides at ambient and higher temperatures [9]. Merkel *et al.* studied the solubility and permeability of light gases, 2 hydrocarbons, and fluorocarbons in a glassy random copolymer of polytetrafluoroethylene and poly (2, 2-bis (trifluoromethyl)-4, 5-difluoro-1, 3-dioxole) (AF2400®) from 25 to 45 °C [10]. Gameda *et al.* elucidated the mixed gas sorption of  $\text{CO}_2/\text{CH}_4$  in polymer of intrinsic microporosity (PIM-1) in between 25 and 50 °C [11]. Stevens *et al.* reported the decrement in gas solubilities with increment in temperature at varying thermally rearranged (TR) polymeric membranes [12].

Based on review of published literature, it is found that many transport property studies include only permeability measurements near ambient conditions. Complementary information on the individual contributions of the sorption and diffusion coefficients to the overall performance at non-ambient and elevated temperatures is rarely reported. The condition thereby limits the availability of data necessary to understand, at a fundamental level, membrane performance at temperatures away from ambient operating conditions. In addition, the systematic studies on temperature dependency of gas transport properties are often obscure, whereby the effect of temperature to different gas penetrants has arrived in contrary and diverging values. In this context, molecular simulation has been proposed as a feasible and complementary alternative of experimentally studied materials to provide insights into gas transport characteristic from an atomistic point of view, usually achieved via a coupling of molecular dynamics (MD) and Monte Carlo (MC) technique. In this context, adaptation of molecular simulation tool overcomes the barrier, cost and time in preparation and



A single polymer chain with 20 repeat units is constructed. The initial polymeric chain has been located in the Forcite module of Materials Studio 8.0 and has been subjected to energy minimization and geometry optimization. The COMPASS force field has been adopted alongside the smart algorithm, which is a combination of the steepest descent; adjusted basis set Newton-Raphson (ABNR) and quasi-Newton algorithms in a cascading manner, in order to refine geometry of the initial polymeric chain. Later, the polymeric membrane chain has been folded into Amorphous Cell module adopting Construction task. The polymer chains have been embedded in the hypothetical cell under the periodic condition at initial density corresponding to 70% of the targeted experimental density ( $1.24 \text{ g/cm}^3$ ) [16]. Similarly, the COMPASS force field has been adopted to pack the polymeric chains.

Subsequently, the PSF structure has been treated adopting the molecular treatment procedure as highlighted in our previous work [17]. The NPT-NVT protocol has been repeated until changes in the successive density values are within predefined tolerance. Thereafter, in order to simulate the effect of operating temperatures to the molecular structure of PSF polymeric membrane, the procedures are repeated at temperature of 308.15 K, 313.15 K and 323.15 K instead of 298.15 K.

## 2.2 Glass Transition Temperature

In this study  $T_g$ s of PSF samples have been determined by mimicking the heating and cooling protocols in laboratory scale adapting a series of thermodynamic treatment in Forcite Module. Firstly, the optimized and equilibrated configuration has been subjected to an additional Canonical (NVT) ensemble at designated operating temperature with a time step of 1 fs and total simulation time of 10 ps by framing the output every 1000 steps. This procedure is aimed to obtain the trajectory files of PSF polymeric films with 10 frames for each operating temperature, such that an average  $T_g$  can be deduced to increase accuracy of the computed value when the series of thermodynamic treatment is iterated while calculating an independent  $T_g$  for each frame. Then, the individual frame located within the PSF trajectory has been exposed to gentle heating from 353.15 K to 553.15 K, which surpasses that of the bulk glass transition temperature of PSF polymer, with an interval of 1 K. Subsequently, a 100 ps NPT dynamic ensemble has been conducted at the designated heating temperature and operating pressure. Thereafter, the system is cooled down from 553.15 K to 353.15 K with the temperature interval of 1 K while computing density of the structure at each temperature. This protocol is looped over all frames contained in the trajectory file and eventually the values are averaged at the end.

## 2.3 Gas Transport Properties

In order to elucidate transport properties of penetrants within the simulated PSF polymer films, gas molecules of  $\text{O}_2$ ,  $\text{N}_2$ ,  $\text{CH}_4$  and  $\text{CO}_2$  have been generated. Analogously, they have been treated with energy minimization and geometry optimization prior to incorporation within the simulated polymeric matrix. Later, the transport

properties of gases, which are of paramount interest to determine separation performance of polymeric membranes, comprising of diffusivity, solubility, and permeability characteristics have been studied. The procedure and underlying theory supporting the evaluation of transport behavior are elaborated in this subsection.

### 2.3.1 Gas Diffusivity

In current work, the diffusivity of gas penetrants has been determined adopting the means of molecular positioning theory, or more commonly known as the Einstein relationship [18–24]. In Einstein correlation, he related the self-diffusion coefficient of gas particles  $i$ ,  $D_i$  to the mean square displacement (MSD) as a function of observation time, such as that presented in (1), through the assumption of particle random walk [25].

$$D_i = \frac{1}{6N} \lim_{t \rightarrow \infty} \frac{d}{dt} \sum_{t=1}^N \langle |r_i(t)^2 - r_i(0)^2| \rangle \quad (1)$$

$N$  is resemblance of the total number of diffusing atoms  $i$  within the hypothetical cell under consideration,  $r_i$  is the position vector of atom  $i$ ,  $|r_i(t)^2 - r_i(0)^2|$  represents ensemble averages of the gas particles MSD, while  $r_i(t)$  and  $r_i(0)$  depicts the final and initial position vector of the centre of mass of gas molecule over the time span of interest,  $t$ . Based on (1), the gas diffusivity coefficient can be analysed from the slope of mean-squared displacement against simulation time, divided by 6.

Subsequently, in order to simulate diffusivities, 10 molecules of each gas species are incorporated within the optimized and equilibrated PSF films, as prepared in Sect. 2.1 of present study. 10 gas molecules have been simulated to collect sufficient trajectory in order to validate a reasonable and accurate pathway of penetrants within the polymeric matrix. Each of the gas molecules has been assigned with a centroid of centre of mass before being embedded inside the hypothetical cell of interest in order to track its respective pathway. Initially, the gas molecules together with the final optimized membrane structure have been subjected to an additional 1000 ps isothermal-isobaric ensemble (NPT) molecular dynamics run to obtain the equilibrated configuration of the gas/polymer system at 2 atm and designated operating temperatures. When approaching the end of dynamic run, an additional Canonical (NVT) simulation has been performed for 2 ns to elucidate the detailed trajectory of the gas molecules. A time step of 1 fs has been employed consistently throughout the simulation process to increase the frequency of consecutive motion of diffusing gas. Ultimately, the MSD computed as a function of time was analyzed using conventional and log–log plots.

### 2.3.2 Gas Solubility

Solubility of the mentioned gases dedicated to  $O_2$ ,  $N_2$ ,  $CO_2$  and  $CH_4$  in PSF polymeric films have been investigated employing the adsorption isotherm task located in Sorption module of Materials Studio 8.0. The embedded adsorption isotherm simulation allows end users to perform a series of grand canonical Monte Carlo ensemble (GCME), in which fugacities of all related components and temperature of the hypothetical system are remained constant. In this simulation work, the gas penetrants have

been incorporated within the equilibrated cell adopting the Metropolis methodology since it has been demonstrated in previous published molecular simulation works to be an adequate characterization for system with relatively small sorbates as compared to pore size of the polymeric matrix and inherits low degree of torsion flexibility, which are highly applicable to gas molecules such as O<sub>2</sub>, N<sub>2</sub>, CO<sub>2</sub> and CH<sub>4</sub> [23, 26]. The GCME in sorption module has been executed for 100 fugacity steps between 0.00001 to 101.325 kPa in equidistant steps. At each pressure, 100000 steps of GCMC calculation are carried out with an initial equilibration period of 10000 steps.

Most simulation techniques are inclined towards determining the condition at infinite dilution and relating it to the solubility coefficient, such as that depicted in (2) [23, 27–29].

$$S_i = \lim_{f_i \rightarrow 0} \left( \frac{C_i}{f_i} \right) = k_{D_i} + c'_{H_i} b_i \quad (2)$$

Hence, in this work, the solubility coefficient,  $S_i$ , has been found through slope of the straight line connecting a point on the solubility isotherm to the origin. In (2),  $C_i$  is the total concentration of gas in the polymer,  $b_i$  and  $C'_{H_i}$  is the Langmuir hole affinity parameter and the capacity parameter respectively, while  $f_i$  is fugacity.

### 2.3.3 Gas Permeability

Permeability is one of the gas transport properties behaviors, which is related to diffusivity and solubility. Permeability is obtained from the product of diffusion coefficient,  $D_i$  and solubility constant,  $S_i$ , as shown below in (3) [15, 30–32].

$$P_i = S_i D_i \quad (3)$$

## 3 Results and Discussion

In this section, the molecular simulation results related to PSF polymeric membranes at different operating temperatures have been presented, whereby it has been subdivided into two major subcategories, such as (1) molecular structure and physical property and (2) gas transport properties.

### 3.1 Molecular Structure and Physical Property

As described in Sect. 2.1, molecular dynamics simulation has been executed for all PSF polymeric films by keeping the operating parameters at the designated operating temperature condition, while the other configurations are constantly updated in quest of determining the most probable polymeric membrane film. Since the structure has been initialized from a lower targeted experimental density, without setting any confinements throughout the molecular dynamics treatment, the evolution of density towards a constant value provide phenomenological interpretation that the constructed molecular

cells have converged to a metastable state. Example of the finalized and optimized PSF membrane, as well as progression of density during the MD process is provided in Fig. 2 (a) and (b) respectively.

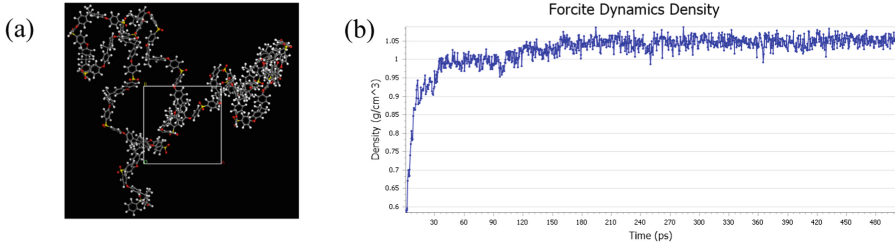


**Fig. 2.** The schematic diagram of (a) equilibrated and optimized PSF polymeric membrane cell and (b) alteration in molecular density.

In this work, the simulated densities at varying operating temperatures have been compared to the Tait equation [33] and Zoller’s correlation [34, 35], such as that depicted in (4), which has been demonstrated to be particularly successful to provide a convenient mathematical characterization of pressure-volume-temperature (PVT) behavior for PSF membranes over a wide range of operating conditions.

$$V(P, T) = 0.8051 + 1.756 \times 10^{-4} T \left\{ 1 - 0.089 \ln \left[ 1 + \frac{P}{4408 \exp(-1.543 \times 10^{-3} T)} \right] \right\} \quad (4)$$

Whereby  $V(P, T)$  represents the specific volume of the polymer at a particular temperature,  $T$ , and pressure,  $P$ , of interest.

Table 1 shows the comparison between densities by using Tait-Zoller’s calculation and this work simulation calculation.

**Table 1.** Comparison of calculated density by using Tait-Zoller formula and simulation.

Temperature (K)	Density (g/cm <sup>3</sup> ) [Experimental correlation]	Density (g/cm <sup>3</sup> ) [This work]	Percentage error (%)
298.15	1.235	1.220	1.21
308.15	1.233	1.211	1.78
313.15	1.231	1.205	2.11
323.15	1.229	1.198	2.52

From the comparison of density between the experimental values, formula calculation and simulated values, it is observed that the deviations are consistently less than 3%. Tentatively, it is found that the molecular simulation tool is of sufficient capability to capture the trend characterizing effect of operating temperature to the density of

molecular structure, such that the density decreases with increment in temperature. The observation can be rationalized through expansion of the simulation cell when operating temperature is raised attributed to higher activation energy for relaxation [34, 35]. Deviation between simulated and experimentally observed PSF density can be explained through the assumption in molecular simulation, whence cut off distance has been applied that deemed long range molecular interaction to be negligible.

In this study, the optimized configuration of the built PSF was heated from temperature of 353.15 K to 553.15 K to obtain the glass transition temperature, whereby the trend of density versus temperature has been plotted in Fig. 3.

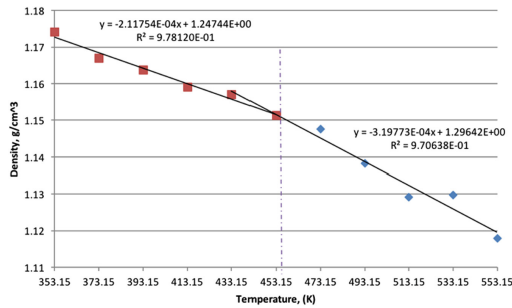


**Fig. 3.** Graph of density against temperature to obtain glass transition temperature.

As it can be seen from Fig. 3, initially the density decreases linearly with increment in temperature, and then shows an abrupt alteration in the value before continuing to embark in another linear region. Change in linear relationship is demonstrated through the difference in slope between the two curves, whereby the first at lower temperature is representative of the glassy state region, while the latter describes the rubbery state. The point at which the glassy and rubbery linear correlation meets to form an intercept provides graphical representation of  $T_g$ . The intersected point at 454.94 K is  $T_g$  obtained from current simulated work. When comparing the obtained  $T_g$  through this simulation, to literature record of 460.15 K [23], the error is at  $-1.13\%$ . Thus, it can be said that the proposed methodology is reliable to obtain molecule structures of high accuracy, before applying in subsequent section to study the gas transport properties at varying operating temperatures.

### 3.2 Gas Transport Properties

In this section, the results pertaining to molecular simulation of PSF polymeric membranes at different operating temperature is presented from the aspect of transport behaviour evolution associated to the temperature, followed by integration of existing correlations to quantify the effect.

### 3.2.1 Gas Diffusivities

The example of mean square displacements (MSDs) for gas penetrants, O<sub>2</sub>, N<sub>2</sub>, CO<sub>2</sub> and CH<sub>4</sub> within PSF polymeric matrix at 308.15 K are summarized in Fig. 4. The mean square displacement is found to increase in a relatively linear manner with time, suggesting that the collected data are of sufficient reliability to constitute the diffusivity data, which would be determined from slope of the graph.

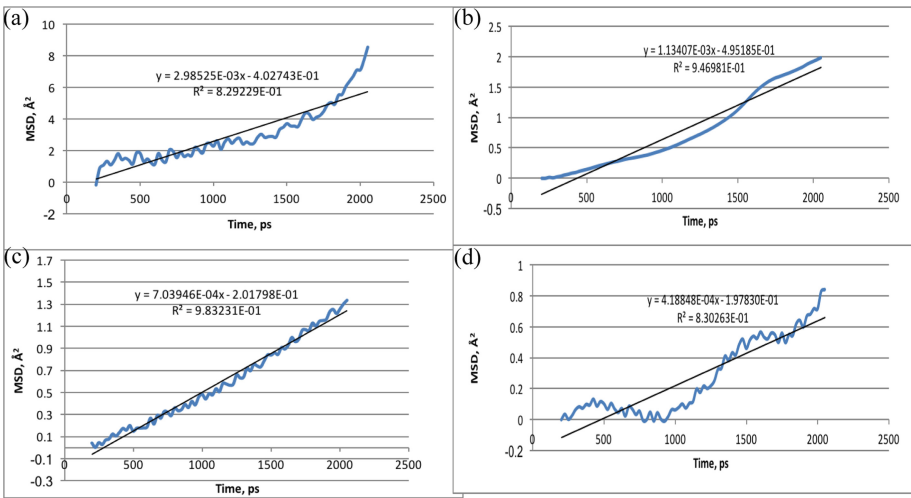


**Fig. 4.** Graph of mean squared displacement (MSD) against time at 308.15 K for (a) O<sub>2</sub> (b) N<sub>2</sub> (c) CO<sub>2</sub> and (d) CH<sub>4</sub>.

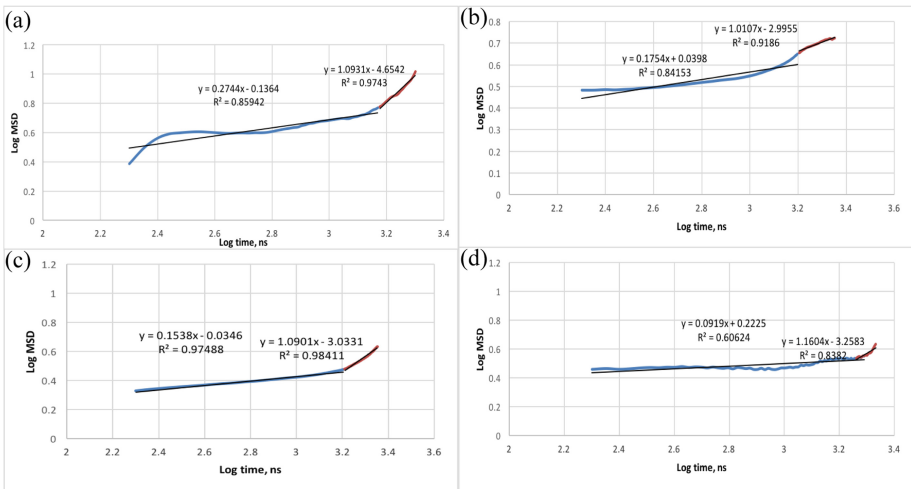


**Fig. 5.** Graph of logarithmic MSD against time for (a) O<sub>2</sub> (b) N<sub>2</sub> (c) CO<sub>2</sub> and (d) CH<sub>4</sub>.

In order to demonstrate that the selected time regime is of sufficient accuracy to characterize the consecutive motion of gas molecules, the logarithmic plot of MSD versus time has been provided in Fig. 5.

When approaching approximately 1500 ps (Log time  $\approx 3.2$ ), an apparent change in slope of the curve has been observed for all gas penetrants and approaching unity at the end of the simulation (e.g. 1.0931 from 0.2744 for O<sub>2</sub>; 1.0107 from 0.1754 for N<sub>2</sub>; 1.0901 from 0.1538 for CO<sub>2</sub> and 1.1604 from 0.09199 for CH<sub>4</sub>). Similar observation has been reported in previous simulation work by Cuthbert *et al.* who observed a slope of 1 when the gas penetrants reached the diffusive regime [36]. Therefore, it is concluded that the allocated simulation time of 2000 ps is appropriate and sufficiently long to capture the diffusive behavior of all gas penetrants in the studied membranes.

The computed diffusivity data at varying operating temperatures for the gas penetrants are tabulated in Table 2.

**Table 2.** Simulated diffusivity for O<sub>2</sub>, N<sub>2</sub>, CO<sub>2</sub> and CH<sub>4</sub> at 298.15 K, 308.15 K, 313.15 K and 323.15 K.

Temperature (K)	Diffusivity ( $\times 10^{-8}$ cm <sup>2</sup> /s)			
	O <sub>2</sub>	N <sub>2</sub>	CO <sub>2</sub>	CH <sub>4</sub>
298.15	4.064	1.542	1.013	0.541
308.15	4.590 (4.2) <sup>a</sup>	1.741 (1.2) <sup>a</sup>	1.112 (1.19) <sup>a</sup>	0.616 (0.27) <sup>a</sup>
313.15	4.975	1.890	1.173	0.698
323.15	5.319	2.039	1.218	0.775

<sup>a</sup>The number in bracket is the experimental value by Ahn *et al.* [16]

Accuracy of the simulated diffusivity data has been verified through comparison between simulation and experimental measured results by Ahn *et al.* [16] at 308.15 K, whereby a small deviation between the two conditions has been observed consistently for all gas penetrants. As it can be seen in Table 2, as the temperature increases, the diffusion coefficient is also increasing. The contributing factor is free volume within the structure of the polymer has increased as the temperature is further increased [37]. Once the free volume of a polymer increases, it allows higher diffusivity of bigger molecules to have a bigger energy to pass through.

It is found that slope of the linear correlation and subsequently diffusion coefficients are similarly in the order of O<sub>2</sub> > N<sub>2</sub> > CO<sub>2</sub> > CH<sub>4</sub>. Such results have been rationalized through the ability of gas molecules to enhance their energy through collision with membrane polymeric chains to jump to neighboring pathway with an appropriate size in order to accommodate their new trajectory. The findings are consistent with various published reports on the diffusivity of gas molecules through polysulfone membranes [16, 38–40]. It has been reported that oxygen is the species that gain most energy and have the energy to execute longest diffusional jump among all penetrants [23].

The impact of operating temperature to gas diffusivity has been quantified through an Arrhenius correlation, as shown in (5), whereby a good fit has been obtained with sufficiently good R<sup>2</sup> for all gas penetrants.

$$D_i = D_{0,i}e^{-\frac{E_{d,i}}{RT}} \tag{5}$$

In (5),  $E_{d,i}$  is the diffusion activation energy,  $D_{0,i}$  is the temperature independent pre-exponential factor and  $R$  is the universal gas constant. The plot of diffusivity as a function of Arrhenius relationship has been provided in Fig. 6.

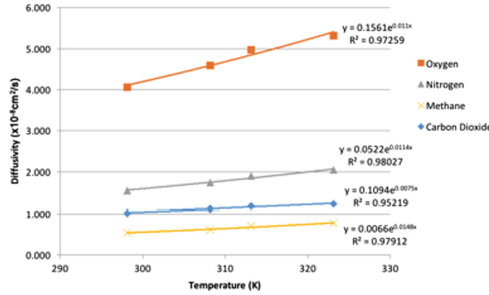


**Fig. 6.** Graph of diffusivity against temperature for O<sub>2</sub>, N<sub>2</sub>, CO<sub>2</sub>, and CH<sub>4</sub> as an exponential function characterizing the Arrhenius correlation (Expression 5).

### 3.2.2 Gas Solubilities

The solubility coefficients can be determined from slope of the concentration curve versus pressure when approaching the zero pressure limits. The example at temperature of 308.15 K for all gas molecules has been provided in Fig. 7, while all the simulated data at varying operating temperatures are summarized in Table 3.

It can be seen that the solubility decreases with increment in temperature attributed to the nature of gas molecules to sustain in its gas state rather than being sorbed within

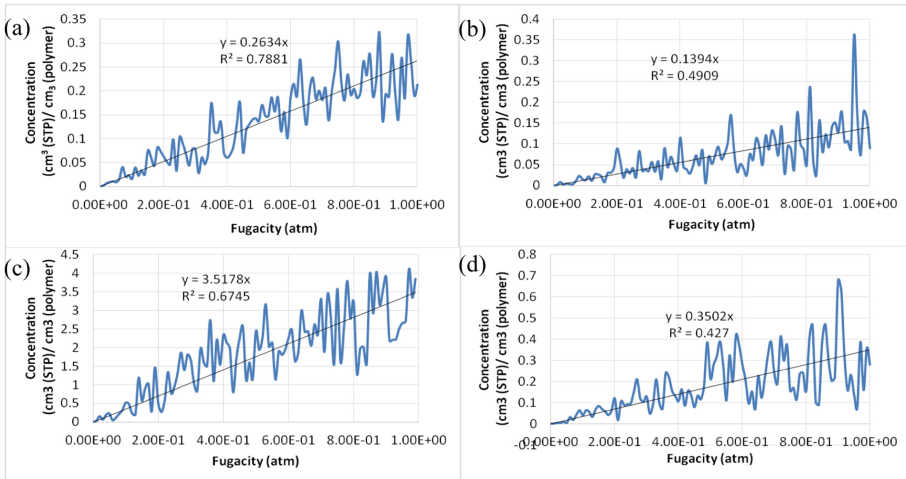


**Fig. 7.** Graph of concentration against fugacity at 308.15 K for (a) O<sub>2</sub> (b) N<sub>2</sub> (c) CO<sub>2</sub> and (d) CH<sub>4</sub>.

**Table 3.** Simulated solubility for O<sub>2</sub>, N<sub>2</sub>, CO<sub>2</sub> and CH<sub>4</sub> at 298.15 K, 308.15 K, 313.15 K and 323.15 K.

Temperature (K)	Solubility (cm <sup>3</sup> (STP)/cm <sup>3</sup> atm)			
	O <sub>2</sub>	N <sub>2</sub>	CO <sub>2</sub>	CH <sub>4</sub>
298.15	0.313	0.177	3.951	0.403
308.15	0.263 (0.25) <sup>a</sup>	0.139 (0.15) <sup>a</sup>	3.518 (4.02) <sup>a</sup>	0.350 (0.27) <sup>a</sup>
313.15	0.239	0.130	2.996	0.281
323.15	0.185	0.099	2.339	0.204

<sup>a</sup>The number in bracket is the experimental value by Ahn *et al.* [16]

the polymeric matrix at higher operating temperature. In a similar manner, the simulated solubility values are found to demonstrate good accordance with experimentally reported data by Ahn *et al.* [16].

The solubility coefficients, are in the order of CO<sub>2</sub> > CH<sub>4</sub> > O<sub>2</sub> > N<sub>2</sub>. Similarly, the trend in gas solubilities in PSF membranes is in good conformity with previous published literatures [16, 38–40]. The good accordance is found to be related to the critical temperature of the gas penetrants, whereby CO<sub>2</sub> with a critical temperature of 304.15 K is highly condensable within the polymeric matrix in comparison to CH<sub>4</sub> (190.56 K), followed by oxygen (154.55 K) and subsequently nitrogen (126.2 K) [41, 42]. Solubility always favors those of higher critical temperature since it indicates ease of gas penetrants to liquefy within the polymer.

In addition, solubility is reported to tally with the Arrhenius calculation with respect to operating temperature based on previous published literatures [12, 23], such as that demonstrated (6).

$$S_i = S_{0,i}e^{-\frac{\Delta H_{S,i}}{RT}} \tag{6}$$

In which  $S_{0,i}$  and  $H_{S,i}$  characterize the temperature independent pre-exponential constant and enthalpy of dissolution respectively. The characterization of gas solubility based on expression (6) is provided in Fig. 8.

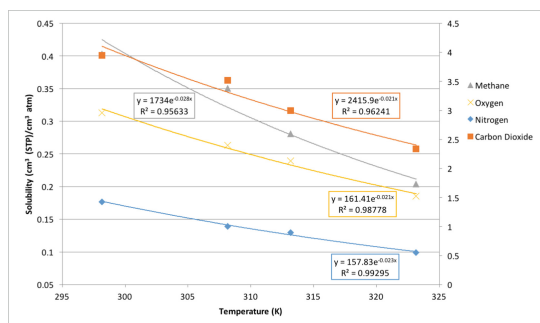


**Fig. 8.** Graph of solubility against temperature for O<sub>2</sub>, N<sub>2</sub>, CO<sub>2</sub>, and CH<sub>4</sub> as an exponential function characterizing the Arrhenius correlation (Expression 6).

### 3.2.3 Gas Permeabilities

The gas permeabilities as a product of diffusivities and solubilities have been calculated and provided in Table 4, while validated with published experimental results by Ahn *et al.* [16].

**Table 4.** Simulated permeability for O<sub>2</sub>, N<sub>2</sub>, CO<sub>2</sub> and CH<sub>4</sub> at 298.15 K, 308.15 K, 313.15 K and 323.15 K.

Temperature (K)	Permeability (Barrer, $\times 10^{-10}$ cm <sup>3</sup> /cm <sup>2</sup> s.cmHg)			
	O <sub>2</sub>	N <sub>2</sub>	CO <sub>2</sub>	CH <sub>4</sub>
298.15	1.271	0.273	4.002	0.218
308.15	1.209 (1.4) <sup>a</sup>	0.243 (0.24) <sup>a</sup>	3.912 (6.3) <sup>a</sup>	0.216 (0.22) <sup>a</sup>
313.15	1.190	0.246	3.515	0.196
323.15	0.986	0.202	2.849	0.158

<sup>a</sup>The number in bracket is the experimental value by Ahn *et al.* [16]

Theoretically, it is found that gas permeability decreases with temperature, which has been rationalized through the rapid decrement in gas solubility as reported in previous section that surpasses the effect of increment in diffusivity. Similar behavior has been observed in previous published work [43].

## 4 Conclusion

This simulation work has shown how affected the membrane polymer are as the operating temperature varies from one to another. It is observable from the modeling structure that the configurations are rather affected. Thus, the first objective of this work, which is the assembling of a sequence of molecular modeling procedure to simulate experimentally validated membrane structures at different operating temperatures, has been successfully achieved. Other than that, it can be concluded that the transport properties are hugely affected by the changing in operating temperature. The diffusivity has shown a positive change in increased temperatures but solubility has shown a decrement in its coefficient as the temperature increases. Permeability is also affected by this whereby it decreases as the temperature increases due to the solubility gaining dominance over diffusivity. Hence, the second objective of this work of elucidating the transport properties of membrane structures at different operating temperatures has also been accomplished. By conducting simulation onto this case study, it has contributed in terms of time saving and cost saving in determining the effects rather than having a lot of time to conduct an experiment. Simulation studies has proven to be another reliable alternative to study the microscopic details of a polymer and its effects as it has been compared that there is no significant variance to the experimental values from literature records. In addition, individual contributions of the sorption and diffusion coefficients to the overall permeability performance at varying operating conditions can be obtained conveniently since it provides phenomenological information towards the correlation between membrane morphology and gas transport properties.

Therefore, it is hopeful to apply this methodology in further studies so that temperature dependent gas transport properties can be further elucidated and quantified to assist in design of separative performance within existing and next-generation polymeric membranes.

**Acknowledgement.** This work is done with the financial support from Universiti Teknologi PETRONAS.

## References

1. Solarin, S.A., Shahbaz, M.: Natural gas consumption and economic growth: the role of foreign direct investment, capital formation and trade openness in Malaysia. *Renew. Sustain. Energy Rev.* **42**, 835–845 (2015)
2. Liang, F.Y., Ryvak, M., Sayeed, S., Zhao, N.: The role of natural gas as a primary fuel in the near future, including comparisons of acquisition, transmission and waste handling costs of as with competitive alternatives. *Chem. Cent. J.* **6**, 1–24 (2012)
3. Baker, R.W., Lokhandwala, K.: Natural gas processing with membranes: an overview. *Ind. Eng. Chem. Res.* **47**, 2109–2121 (2008)
4. U.G. Limited: Chemical Composition of Natural Gas (2017)
5. Lock, S.S.M., Lau, K.K., Ahmad, F., Shariff, A.M.: Modeling, simulation and economic analysis of CO<sub>2</sub> capture from natural gas using cocurrent, countercurrent and radial crossflow hollow fiber membrane. *Int. J. Greenh. Gas Control* **36**, 114–134 (2015)
6. Safari, M., Ghanizadeh, A., Montazer-Rahmati, M.M.: Optimization of membrane-based CO<sub>2</sub>-removal from natural gas using simple models considering both pressure and temperature effects. *Int. J. Greenh. Gas Control* **3**, 3–10 (2009)
7. Costello, L.M., Koros, W.J.: Temperature dependence of gas sorption and transport properties in polymers: measurement and applications. *Ind. Eng. Chem. Res.* **31**, 2708–2714 (1992)
8. Koros, W.J., Paul, D.R.: CO<sub>2</sub> sorption in poly(ethylene terephthalate) above and below the glass transition. *J. Polym. Sci., Part B: Polym. Phys.* **16**, 1947–1963 (1978)
9. Costello, L.M., Koros, W.J.: Thermally stable polyimide isomers for membrane-based gas separations at elevated temperatures. *J. Polym. Sci., Part B: Polym. Phys.* **33**, 135–146 (1995)
10. Merkel, T.C., He, Z., Pinnau, I., Freeman, B.D., Meakin, P., Hill, A.J.: Sorption and transport in Poly(2,2-bis(trifluoromethyl)-4,5-difluoro-1,3-dioxole-co-tetrafluoroethylene) containing nanoscale fumed silica. *Macromolecules* **36**, 8406–8414 (2003)
11. Gameda, A.E., De Angelis, M.G., Du, N., Li, N., Guiver, M.D., Sarti, G.C.: Mixed gas sorption in glassy polymeric membranes. III. CO<sub>2</sub>/CH<sub>4</sub> mixtures in a polymer of intrinsic microporosity (PIM-1): effect of temperature. *J. Membr. Sci.* **524**, 746–757 (2017)
12. Stevens, K.A., Smith, Z.P., Gleason, K.L., Galizia, M., Paul, D.R., Freeman, B.D.: Influence of temperature on gas solubility in thermally rearranged (TR) polymers. *J. Membr. Sci.* **533**, 75–83 (2017)
13. Barnard, A., Li, C.M., Zhou, R., Zhao, Y.: Modelling of the nanoscale. *Nanoscale* **4**, 1042–1043 (2012)
14. Accelrys Software Inc. (2015)
15. Freeman, B.D., Pinnau, I.: Polymeric materials for gas separations. In: *Polymer Membranes for Gas and Vapor Separation*, pp. 1–27. American Chemical Society (1999)

16. Ahn, J., Chung, W.-J., Pinnau, I., Guiver, M.D.: Polysulfone/silica nanoparticle mixed-matrix membranes for gas separation. *J. Membr. Sci.* **314**, 123–133 (2008)
17. Lock, S.S.M., Lau, K.K., Mei, I.L.S., Shariff, A.M., Yeong, Y.F.: Cavity energetic sizing algorithm applied in polymeric membranes for gas separation. *Proc. Eng.* **148**, 855–861 (2016)
18. Hu, N., Fried, J.R.: The atomistic simulation of the gas permeability of poly(organophosphazenes). Part 2. Poly[bis(2,2,2-trifluoroethoxy)phosphazene]. *Polymer* **46**, 4330–4343 (2005)
19. Liu, Q.L., Huang, Y.: Transport behavior of oxygen and nitrogen through organasilicon-containing polystyrenes by molecular simulation. *J. Phys. Chem. B* **110**, 17375–17382 (2006)
20. Wang, X.-Y., Raharjo, R.D., Lee, H.J., Lu, Y., Freeman, B.D., Sanchez, I.C.: Molecular simulation and experimental study of substituted polyacetylenes: fractional free volume, cavity size distributions and diffusion coefficients. *J. Phys. Chem. B* **110**, 12666–12672 (2006)
21. Follain, N., Valleton, J.-M., Lebrun, L., Alexandre, B., Schaezel, P., Metayer, M., Marais, S.: Simulation of kinetic curves in mass transfer phenomena for a concentration-dependent diffusion coefficient in polymer membranes. *J. Membr. Sci.* **349**, 195–207 (2010)
22. Hertäg, L., Bux, H., Caro, J., Chmelik, C., Remsungnen, T., Knauth, M., Fritzsche, S.: Diffusion of CH<sub>4</sub> and H<sub>2</sub> in ZIF-8. *J. Membr. Sci.* **377**, 36–41 (2011)
23. Golzar, K., Amjad-Iranagh, S., Amani, M., Modarress, H.: Molecular simulation study of penetrant gas transport properties into the pure and nano sized silica particles filled polysulfone membranes. *J. Membr. Sci.* **451**, 117–134 (2014)
24. Budhathoki, S., Shah, J.K., Maginn, E.J.: Molecular simulation study of the solubility, diffusivity and permselectivity of pure and binary mixtures of CO<sub>2</sub> and CH<sub>4</sub> in the ionic liquid 1-n-Butyl-3-methylimidazolium bis(trifluoromethylsulfonyl)imide. *Ind. Eng. Chem. Res.* **54**, 8821–8828 (2015)
25. Nagar, H., Vadthya, P., Prasad, N., Sridhar, S.: Air separation by facilitated transport of oxygen through a Pebax membrane incorporated with a cobalt complex. *RSC Adv.* **5**, 76190–76201 (2015)
26. Siepmann, J.I., Frenkel, D.: Configurational bias Monte Carlo: a new sampling scheme for flexible chains. *Mol. Phys.* **75**, 59–70 (1992)
27. Anderson, K.E., Siepmann, J.I.: Molecular simulation approaches to solubility. In: Letcher, T.M. (ed.) *Developments and Applications in Solubility*, pp. 171–177. R. Soc. Chem., Cambridge (2007)
28. Jiang, Y., Willmore, F.T., Sanders, D., Smith, Z.P., Ribeiro, C.P., Doherty, C.M., Thorton, A., Hill, A.J., Freeman, B.D., Sanchez, I.C.: Cavity size, sorption and transport characteristics of thermally rearranged polymers. *Polym.* **52**, 2244–2254 (2011)
29. De Angelis, M.G.: Solubility coefficient (S). In: Drioli, E., Giorno, L. (eds.) *Encyclopedia of Membranes*, pp. 1–5. Springer, Berlin (2015). doi:[10.1007/978-3-642-40872-4\\_631-1](https://doi.org/10.1007/978-3-642-40872-4_631-1)
30. Alexander, S.S.: Polymers for gas separations: the next decade. *J. Membr. Sci.* **94**, 1–65 (1994)
31. Ghosal, K., Freeman, B.D.: Gas separation using polymer membranes: an overview. *Polym. Adv. Technol.* **5**, 673–697 (1994)
32. Freeman, B.D., Pinnau, I.: *Polymer Membranes for Gas and Vapor Separation*. American Chemical Society, Washington, D.C. (1999)
33. Tait, P.G.: Report on some of the physical properties of fresh water and sea, Report on the scientific results of the voyage of the H.M.S. Challenger during the years 1873–1876. *Phys. Chem.* **2**, 1–76 (1988)

34. Zoller, P.: Specific volume of polysulfone as a function of temperature and pressure. *J. Polym. Sci., Part B: Polym. Phys.* **16**, 1261–1275 (1978)
35. Zoller, P.: A study of the pressure-volume-temperature relationships of four related amorphous polymers: polycarbonate, polyarylate, phenoxy, and polysulfone. *J. Polym. Sci., Part B: Polym. Phys.* **20**, 1453–1464 (1982)
36. Cuthbert, T.R., Wagner, N.J., Paulaitis, M.E., Murgia, G., D'Aguanno, B.: Molecular dynamics simulation of penetrant diffusion in amorphous polypropylene: diffusion mechanisms and simulation size effects. *Macromolecules* **32**, 5017–5028 (1999)
37. Robeson, L.M.: Polymer membranes for gas separation. *Curr. Opin. Solid State Mater. Sci.* **4**, 549–552 (1999)
38. McHattie, J.S., Koros, W.J., Paul, D.R.: Gas transport properties of polysulphones: 1. role of symmetry of methyl group placement on bisphenol rings. *Polymer* **32**, 840–850 (1991)
39. Aitken, C.L., Koros, W.J., Paul, D.R.: Effect of structural symmetry on gas transport properties of polysulfones. *Macromolecules* **25**, 3424–3434 (1992)
40. Ghosal, K., Chern, R.T., Freeman, B.D., Daly, W.H., Negulescu, I.I.: Effect of basic substituents on gas sorption and permeation in polysulfone. *Macromolecules* **29**, 4360–4369 (1996)
41. Timmerhaus, K.D.: *Advances in Cryogenic Engineering*. Springer, US (1995). doi:[10.1007/978-1-4613-9847-9](https://doi.org/10.1007/978-1-4613-9847-9)
42. de Oliveira, M.J.: *Equilibrium Thermodynamics*. Springer, Heidelberg (2013). doi:[10.1007/978-3-642-36549-2](https://doi.org/10.1007/978-3-642-36549-2)
43. Ohlrogge, K., Stürken, K.: Membranes: separation of organic vapors from gas streams. In: Ullmann's Encyclopedia of Industrial Chemistry. Wiley-VCH Verlag GmbH & Co. KGaA (2000)